Computers and Electronics in Agriculture 243 (2026) 111428

Contents lists available at ScienceDirect

Computers and Electronics in Agriculture

journal homepage: www.elsevier.com/locate/compag

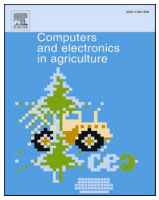

Original papers

OptiDose: An optimal control for macronutrient dosing in hydroponics

Saeed Karimzadeh [a,b,c,*], Robert D. McAllister [b], Md Shamim Ahamed [a,**]

[a] Department of Biological and Agricultural Engineering, University of California, Davis, CA, USA
[b] Delft Center for Systems and Control, Delft University of Technology, Delft, Netherlands
[c] Department of Built Environment, Aalto University, Espoo, Finland

ARTICLE INFO

Keywords:
OptiDose
Optimal control
Nutrient solution optimization
Fertilizer dosing strategy
Precision agriculture
Closed-loop fertigation
Hydroponic lettuce production

ABSTRACT

Achieving closed-loop hydroponics necessitates precise adjustment of individual macro- and micronutrients within the nutrient solution. However, nutrient management in hydroponics remains constrained to electrical conductivity (EC) and pH-based approaches, due to the complexity of steering individual ions and the coupling inherent in multi-element fertilizer formulations. In this study, an optimal control framework, termed *OptiDose*, is implemented to optimize daily fertigation strategies for hydroponically grown lettuce. The system integrates six fertilizer sources—calcium nitrate, magnesium sulfate, monopotassium phosphate, potassium nitrate, magnesium nitrate, and potassium sulfate—to maintain the concentrations of the macronutrients nitrogen (N), phosphorus (P), potassium (K), calcium (Ca), magnesium (Mg), and sulfur (S) within crop-specific adequacy ranges. Five scenarios are tested in the simulator to evaluate system performance under varying operational constraints. Results indicate that *OptiDose* maintained suitable nutrient concentrations for plants throughout the growth cycle—without nutrient deficiencies or toxicities—while markedly improving resource-use efficiency. Relative to a single-shot nutrient preparation (baseline), the strategy using properly sized solution tanks with daily recipe adjustment (Scenario 1) increased water-use efficiency sixfold and doubled fertilizer-use efficiency, achieving 32.3 ± 1.4 g/L and 12.3 ± 0.3 g/g, respectively. Additionally, water and fertilizer costs decreased significantly ($p < 0.05$), by approximately 76% and 51%, respectively. The results underscore the promise of element-specific fertigation and optimization for precision nutrient management in controlled environment agriculture.

1. Introduction

Hydroponics, a form of soilless agriculture, involves cultivating plants in aqueous solutions enriched with essential mineral nutrients, thereby eliminating the need for soil as a growth medium. Hydroponic systems are broadly categorized into two types: open-loop and closed-loop systems. In open-loop systems, the applied nutrient solution is periodically discarded, whereas closed systems collect and recycle nutrient solution, enabling reuse throughout the cultivation cycle (Raviv et al., 2019). The environmental ramifications of open-loop hydroponics are substantial, as the discharge of nutrient-laden effluent can contaminate surrounding ecosystems and groundwater sources (Pandey et al., 2023). In contrast, closed-loop hydroponics has demonstrated a 20–40% reduction in nutrient input requirements (Pandey et al., 2023). In some cases, water and fertilizer inputs can be reduced by 20–35% and 40–50%, respectively, in comparison to conventional open-loop soilless cultivation systems, while substantially minimizing—or in some instances entirely eliminating—nutrient losses to the environment and offering both economic and ecological advantages (Giannothanasis et al., 2024; Grewal et al., 2011; Karimzadeh et al., 2025b,c; Massa et al., 2011). This advancement is critical for mitigating escalating water demand in food production, a challenge intensified by climate change in conventional open-field agriculture (Karimzadeh et al., 2025a).

For optimal growth and productivity, plants require 17 essential elements (Trejo-Téllez and Gómez-Merino, 2012). Of these, carbon (C), hydrogen (H), and oxygen (O) are derived from atmospheric CO_2 and water. The remaining 14 elements must be supplied through the nutrient solution and are classified as macronutrients—nitrogen (N), phosphorus (P), potassium (K), calcium (Ca), magnesium (Mg), and sulfur (S)—and micronutrients—iron (Fe), zinc (Zn), manganese (Mn), copper (Cu), boron (B), molybdenum (Mo), chlorine (Cl), and nickel (Ni) (Kim et al., 2023). Nutrient management in hydroponic systems is conventionally regulated via electrical conductivity (EC) measurements, which serve as a proxy for total ion concentration. Water and nutrient replenishment

* Corresponding author at: Department of Biological and Agricultural Engineering, University of California, Davis, CA, USA.
** Corresponding author.
E-mail addresses: saeed.karimzadeh@aalto.fi (S. Karimzadeh), mahamed@ucdavis.edu (M.S. Ahamed).

https://doi.org/10.1016/j.compag.2026.111428
Received 4 October 2025; Received in revised form 4 January 2026; Accepted 7 January 2026
Available online 13 January 2026

are typically automated, with concentrated fertilizer solutions injected in proportion to fluctuations in EC caused by plant uptake (Bailey et al., 1988). However, EC provides no information on the individual ion concentrations and cannot reflect nutrient-specific imbalances (Kim et al., 2023). Such limitations hinder the precision management of individual nutrient formulations tailored to the dynamic demands of crops.

Advances in sensor networks and fertigation automation offer promising solutions for closed-loop nutrient optimization. Although several studies have demonstrated the viability of automated fertigation systems for soilless cultivation (Domingues et al., 2012; Pandey et al., 2023; Rahman et al., 2018; Steidle Neto et al., 2014), sustaining individual nutrient balance remains a persistent challenge. Conventional monitoring strategies, primarily based on EC and pH measurements (Cho et al., 2017), are insufficient to detect ionic imbalances or the accumulation of non-absorbed solutes, which can arise due to differential uptake rates at the root interface.

Recent advancements in nutrient concentration measurement techniques—including colorimetry, spectrophotometry, ion-selective electrodes (ISEs), and emission spectroscopy (Ahamed et al., 2025; Langenfeld et al., 2022)—have enabled more precise characterization of individual ionic species. ISEs provide real-time, on-site data for immediate nutrient management with moderate accuracy (due to ion interference). Conversely, highly accurate techniques (e.g., emission spectroscopy and ion chromatography) are costly, off-line and laboratory-based, resulting in a considerable time lag for clarifying the nutrient status (Ahamed et al., 2025). These innovations offer unprecedented opportunities to refine nutrient management strategies by aligning nutrient dosing more closely with plant-specific uptake dynamics. One such approach, implemented in the decision support system NUTRISENSE (Giannothanasis et al., 2024, 2025; Savvas et al., 2023), regulates the nutrient solution supplied to plants by analyzing the chemical composition of the drainage solution. This feedback-based strategy aims to align nutrient inputs with crop uptake, thereby maintaining target root-zone concentrations of the required ions. However, the system depends on sequential calculations of individual nutrient mass balances to determine dosing, a process that is both labor-intensive and susceptible to errors. Moreover, it lacks the capacity to predict future nutrient uptake, limiting its ability to adjust dosing proactively over a defined time horizon. A more systematic and scalable approach, such as the matrix-based method proposed by Jung et al. (2015) could streamline these calculations. A 3 × 3 matrix formulation was used to compute the required doses of three fertilizer stock solutions based on their nutrient contribution ratios and ion concentrations to achieve fixed target concentrations for NO_3, K, and Ca. However, this approach does not account for future nutrient demand or dynamic adjustments needed to maintain nutrient concentrations within optimal ranges for plant growth. To date, no widely adopted control algorithm exists that enables optimization of water and fertilizer inputs based on individual nutrient concentrations rather than aggregate EC values. Developing such precision fertigation algorithms would mark a substantial advancement in sustainable and high-efficiency hydroponic crop production.

Agricultural systems are inherently complex and subject to uncertainty (Ding et al., 2018; Kamilaris and Prenafeta-Boldú, 2018). Traditional control strategies, including on/off and proportional-integral-derivative (PID) controllers, are widely used due to their simplicity (Afram and Janabi-Sharifi, 2014; Christofides et al., 2013; Ding et al., 2018). Traditional PID control methods are also unaware of the economic/environmental costs of their actions. Alternatively, fuzzy logic enables adaptive control of nutrient solutions under dynamic cultivation conditions (Catota-Ocapana et al., 2025; Mohamed et al., 2022). Fuzzy logic, in particular, has shown clear advantages over traditional PID control in hydroponics nutrient management. Zhang et al. (2019) reported that fuzzy PID reduced overshoot, improved response time, and enhanced system stability. Other studies (Dela Vega et al., 2021; Nurmahaludin et al., 2020) successfully applied fuzzy logic to regulate pH and EC in nutrient solutions, with the latter incorporating the Sugeno method and servo motor adjustments. Mashumah et al. (2018) combined image processing with fuzzy logic to adjust EC based on plant age, achieving high accuracy. Puno et al. (2020) further expanded on sensor-driven fuzzy logic control systems to manage EC, pH, and water levels; however, their design included draining the mixing tank—a potentially problematic feature due to environmental concerns over nutrient-rich wastewater and the added operational costs for water and fertilizer replenishment. A recent study further revealed that while PID responded faster, fuzzy control minimized overshoot, and consensus algorithms offered the best overall balance (Nizam et al., 2024). Despite their contributions, none of these studies addressed nutrient solution preparation beyond basic EC and pH control. In some cases, overshooting in algorithms led to the implementation of drainage systems (e.g., Puno et al., 2020). Moreover, these methods struggle with dynamic processes involving time delays and require extensive tuning, making them impractical for real-time precision agriculture (Wang et al., 2001), particularly for multiple-input and multiple-output (MIMO) systems with operational constraints.

This study aimed to develop a finite-horizon optimal control framework, termed *OptiDose*, motivated by the need to enable precise regulation of inputs to optimize water and nutrient dosing for lettuce cultivation in hydroponic systems. The model accounted for daily plant uptake dynamics of water and macronutrients (N, P, K, Ca, Mg, and S). The objective of the newly developed algorithm was to minimize resource use (water and fertilizers) while prioritizing the reduction of macronutrient toxicity and deficiency risks for plants throughout the crop growth cycle. Six commonly used fertilizers—calcium nitrate, magnesium sulfate, monopotassium phosphate, potassium nitrate, magnesium nitrate, and potassium sulfate—were incorporated to meet macronutrient requirements. Five distinct farm management scenarios were evaluated, and a suite of standardized performance metrics was used to assess the effectiveness. The study evaluates the potential of *OptiDose* to enhance input-use efficiency and enable individual nutrient level management (addressing the limitations of EC-based approaches) in hydroponic crop production.

2. Materials and methods

The initial step involved developing a comprehensive understanding of plant physiological responses. *OptiDose* (Fig. 1) is fundamentally structured around three core processes: (i) biomass accumulation, (ii) evapotranspiration, and (iii) macronutrient uptake. The first two processes were quantified through controlled experiments and data collection (Section 2.1), while the dynamics of nutrient uptake were derived from existing literature (Section 2.1). Building on these components, the optimization framework was subsequently formulated (Section 2.2). Finally, five scenarios reflecting farmer practices were simulated (Section 2.3) to evaluate system performance (Section 2.4).

2.1. Experimental setup and conditions

The experiment was conducted in an indoor farming facility in the Controlled Environment Engineering Lab at the University of California, Davis, USA (38.54°N, 121.75°W). A closed-loop nutrient film technique (NFT) hydroponic system was employed to cultivate butterhead lettuce (*Lactuca sativa var. capitata*). The channel cross section was rectangular and inclined at 2–4% to facilitate nutrient solution flow from the inlet to the drainage collection pipe (Fig. 2 and Supplementary Video). Fourteen-day-old seedlings, grown in cocopeat, were transplanted into the system on February 22, 2024, and cultivated until harvest on March 22, 2024. The hydroponic system comprised two horizontal trays, each measuring 1.0 × 1.4 m, accommodating a total of 70 lettuce plants at a density of 25 plants per square meter of growing area.

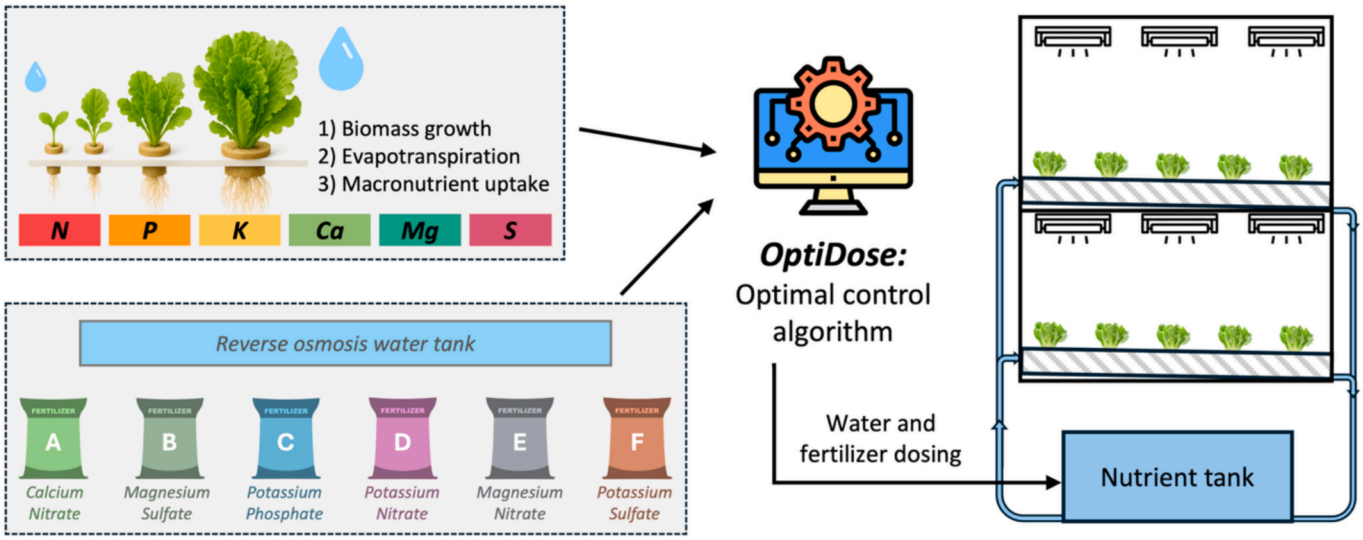

Fig. 1. Overview of the proposed control framework for optimal macronutrient dosing (*OptiDose*) for hydroponic production.

2.1.1. Environmental conditions and lighting

Environmental conditions, including temperature, relative humidity, EC, and nutrient solution volume, were recorded throughout the experiment (Fig. 2b–c). The air temperature exhibited tier-dependent variations, averaging 22.9 ± 2.9°C in the upper tier and 21.6 ± 2.8°C in the lower tier. Relative humidity remained stable at 50 ± 7% in the upper tier and 49 ± 7% in the lower tier. A 16-hour photoperiod was maintained from 08:00 to 24:00, with an irradiance of 250 μmol/m^2/s at the rack center, measured with a LI-180 (LI-COR, USA). The corresponding daily light integral (DLI) was 14.4 mol/m^2/d. Illumination was provided by a total of 12 cool-white fluorescent lamps (6500 K T5; VIVOSUN, USA), with six lamps installed per tray.

2.1.2. Nutrient solution and growth monitoring

The nutrient solution composition was prepared with macronutrient concentrations (mg/L) of N: 176, P: 31, K: 237, Ca: 126, Mg: 15, S: 28. The solution was prepared with calcium nitrate (69.8 g/100 L), magnesium sulfate (15.6 g/100 L), monopotassium phosphate (13.8 g/100 L), and potassium nitrate (51.9 g/100 L) (Table 1), calculated using the *GrowDose*™ nutrient recipe software. It operates by utilizing the nutrient composition indicated on fertilizer labels to precisely compute the quantities required to achieve user-defined macro- and micronutrient target concentrations. Micronutrient concentrations (mg/L) were as follows: B: 0.137, Cu: 0.410, Fe: 0.820, Mn: 0.684, Zn: 1.230. Due to the limited tank capacity (~95 L), the nutrient solution tank was replenished regularly to maintain volume and nutrient balance. Water (10 L per application) was added on February 29 (7 days after transplanting [DAT]), March 4 (11 DAT), March 15 (22 DAT), March 16 (23 DAT), and March 17 (24 DAT). Nutrient solution was applied on March 6 (13 DAT), March 8 (15 DAT), March 10 (17 DAT), March 12 (19 DAT, calcium nitrate only), March 14 (21 DAT), and March 20 (27 DAT). On March 8 (15 DAT) and March 20 (27 DAT), both water and nutrient solution were applied (Table S1). Here, DAT refers to the number of days after transplanting, which occurred on February 22. Daily fresh weight was measured for 18 lettuce heads grown on the lower tier to monitor biomass accumulation. Each measurement included the total weight of the plant (shoot and root) along with the cocopeat substrate. To isolate the net plant biomass, the saturated weight of the substrate was subtracted from the total measured weight.

2.1.3. Sensor calibration and data acquisition

The nutrient solution EC was monitored using a Vernier EC sensor (Vernier, USA), which was calibrated using a two-point calibration method (1 and 50 dS/m). The pH was maintained at ~5.5 through manual adjustments. EC and water level were monitored daily, and nutrient solution adjustments were performed twelve times throughout the growing cycle to maintain optimal conditions (Table S1). Air temperature and relative humidity were measured using DHT22 sensors (AOSONG, China), positioned 30 cm above the center of the growing channels. The sensors provided a temperature accuracy of ±0.5°C and a relative humidity accuracy of ±2% RH (maximum ±5% RH). The water level was installed above the tank and measured using an HC-SR04 ultrasonic sensor (MaxBotix, USA), with an accuracy of up to 3 mm. All sensors were integrated with an Arduino Mega system (Arduino, Italy), enabling continuous data logging at 15-second intervals. The data were then averaged to provide measurements at 30-minute intervals. To mitigate microbial contamination, a UV disinfection system (AQUANEAT, USA) was incorporated into the nutrient solution reservoir. Fig. 2 illustrates the experimental setup alongside the range and variability of key growing parameters (Karimzadeh and Ahamed, 2025).

2.1.4. Biomass and evapotranspiration models

The hydroponic system analyzed in this study was designed to integrate key physiological and biophysical processes, including lettuce

Table 1
List of selected fertilizer compounds used in the nutrient solution formulation, including their chemical names, compositions, and market price (USD/kg).

Fertilizer tank	Fertilizer	Chemical compound	Chemical composition by weight	Price† (USD/kg)
Tank A	Calcium nitrate	$Ca(NO_3)_2$	N-NO_3: 15%, Ca: 18%	11
Tank B	Magnesium sulfate	$MgSO_4$	Mg: 10%, S: 13%	
Tank C	Monopotassium phosphate	KH_2PO_4	P_2O_5: 52%, K_2O: 34%	
Tank D	Potassium nitrate	KNO_3	N-NO_3: 13.7%, K_2O: 46%	
Tank E	Magnesium nitrate	$Mg(NO_3)_2$	N-NO_3: 11%, MgO: 16%, Mg: 9.6%	
Tank F	Potassium sulfate	K_2SO_4	K_2O: 52%, S: 18%	

† Prices from Green Leaf Aquariums, LLC (Gainesville, FL, USA; greenleafaquariums.com), retrieved June 2025.

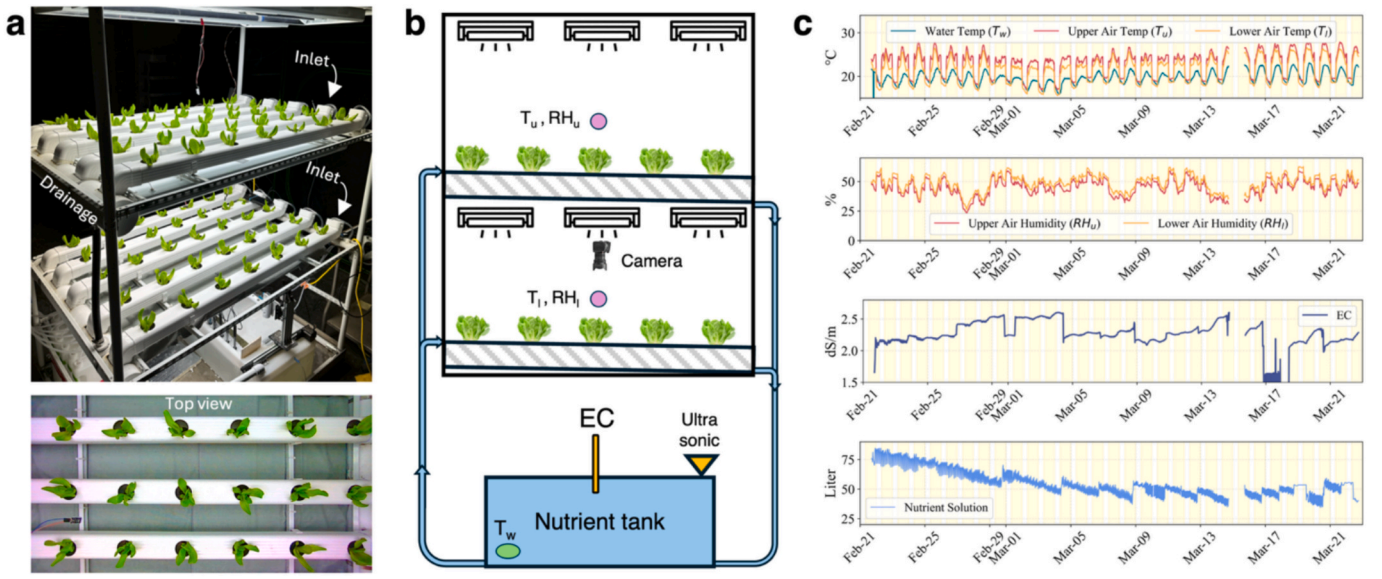

Fig. 2. (a) Lettuce growth on the transplanting date, (b) Schematic of the closed-loop NFT hydroponic system with two vertical tiers in controlled environment agriculture (CEA), (c) Time series of measured parameters: air temperature, humidity, EC, and nutrient solution volume and temperature (Data from Karimzadeh and Ahamed, 2025).

biomass accumulation, evapotranspiration dynamics, and macronutrient uptake kinetics for N, P, K, Ca, Mg, and S. Biomass was the key factor that affected evapotranspiration and nutrient uptake rates. Fig. 3 shows the daily biomass measurements for the 18 lettuce heads in the bottom tier. A sigmoid function was used to model the average biomass per lettuce head:

$$y = \frac{y_{max}}{1 + e^{-r(t-t_0)}} \tag{1}$$

where y_{max} is the 163 g/head, r is the fitted growth rate (0.195), and t_0 is the fitted parameter with a value of 17.5 and t is DAT.

The total cumulative evapotranspiration was ~173 L. Eq. (2) was employed to model the daily crop evapotranspiration ($ET_{c,t}$) as a function of biomass growth and maximum evapotranspiration ($ET_{c,max}$). The model is expressed as:

$$ET_{c,t} = \left(\frac{Biomass_t}{Total\,Biomass}\right).ET_{c,max} + E \tag{2}$$

where E represents pure evaporation from the tank surface (0.3 L/day), measured independently of crop biomass.

2.2. Overview of OptiDose

To facilitate element-specific fertigation that ensures nutrient sufficiency while minimizing water and fertilizer inputs, a nutrient–water optimization framework was developed that integrates lettuce growth forecasting with finite-horizon optimal control to determine optimal dosing strategies. In this framework, the primary model inputs include biomass accumulation, evapotranspiration dynamics, macronutrient uptake rates, and the unit prices of water and fertilizers. *OptiDose* generated the optimal sequence of daily fertigation doses by minimizing a cost function that jointly penalized nutrient imbalances, water overuse, and economic inefficiencies, subject to physiological and operational constraints.

2.2.1. Model formulation

The optimal control problem was formulated over a 30-day prediction horizon, with a daily control resolution. The system comprises seven state variables representing nutrient and water mass (six macronutrients and nutrient solution water), and seven control outputs, which correspond to the application rates of six distinct fertilizers (Table 1) and reverse osmosis water. The state dynamics of the nutrient solution were governed by the discrete-time linear system:

$$x_{t+1} = x_t + B.u_t + d_t + w_t \tag{3}$$

where u_t denotes the control signal output, d_t is the plant nutrient and water uptake profile on day t, described in section 2.1.4, w_t represents the uncertainty associated with plant nutrient uptake (see Section 2.2.3; Table 2).

- $x_t \in \mathbb{R}^7, t \in \{1, 2, \cdots, T\}$: state vector representing mass of nutrients and water volume across T = 30 days.
- $u_t \in \mathbb{R}^7, t \in \{1, 2, \cdots, T-1\}$: control vector (dosing) for six fertilizers and one reserve osmosis water (7 components).
- $d_t \in \mathbb{R}^7, t \in \{1, 2, \cdots, T\}$: vector representing the mass of six macronutrients and water taken up by plants (negative flux), expressed as a function of biomass accumulation (see Section 2.1.4).
- $w_t \in \mathbb{R}^7, t \in \{1, 2, \cdots, T\}$: vector of uncertainties in six macronutrient and water uptake rates (see Table 2).

$B \in \mathbb{R}^{7\times7}$ is the constant transformation matrix encoding fertilizer-to-nutrient mapping, it is based on the chemical composition listed on the labels of the six selected fertilizers (Table 1), as well as the nutrient concentration of the dosing water (zero for reverse osmosis water). Rows represented the seven system states being tracked: 1) N, 2) P, 3) K, 4) Ca, 5) Mg, 6) S, and 7) water. Columns corresponded to the control inputs, which were the volumes (in liters) of six fertilizer stock solutions and water added to the system each day: 1) tank A: calcium nitrate [$Ca(NO_3)_2$], 2) tank B: magnesium sulfate [$MgSO_4$], 3) tank C: monopotassium phosphate [KH_2PO_4], 4) tank D: potassium nitrate [KNO_3], 5) tank E: magnesium nitrate [$Mg(NO_3)_2$], 6) tank F: potassium sulfate [K_2SO_4], 7) tank G: water (no nutrients). Each entry $B_{m,i}$ of the matrix quantifies the amount of nutrient m delivered per liter of solution i. These values were computed based on the fertilizer concentration (50 g dissolved per liter of water) and the nutrient content of each fertilizer (from product specifications).

To accurately quantify the amount of elemental nutrients delivered by each fertilizer source, the nutrient content expressed as oxides (commonly used in fertilizer labeling) was converted to its elemental

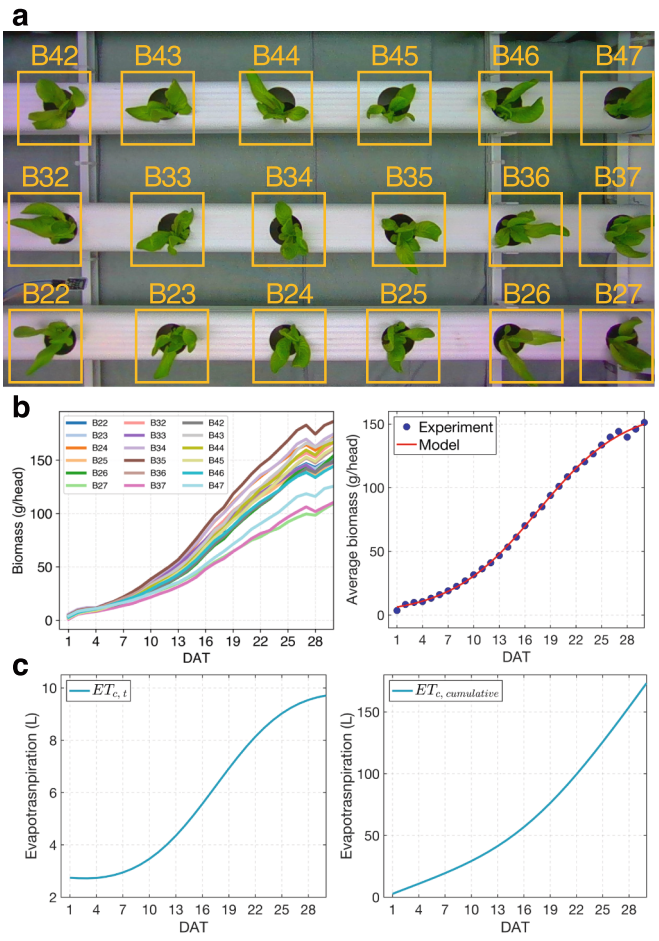

Fig. 3. Monitoring and modeling plant growth and evapotranspiration. (a) Images of the OptiDose: An optimal control for macronutrient dosing in hydroponicsmeasured individual plants across three rows of NFT in the lower tier levels. (b) Biomass accumulation trends during the growing season. Left: Individual plant biomass growth curves. Right: Comparison between experimental average biomass (blue dots) and model-predicted values (red line). (c) Temporal dynamics of evapotranspiration. Left: Daily evapotranspiration rate ($ET_{c,t}$), and right: Cumulative evapotranspiration ($ET_{c,cumulative}$).

equivalents using molecular conversion factors. Oxide-based guaranteed analyses were converted to elemental nutrient mass using stoichiometric (molar-mass) fractions. Specifically, elemental phosphorus was computed as $P = 0.436P_2O_5$, potassium as $K = 0.830K_2O$, and magnesium as $Mg = 0.603MgO$; these factors follow directly from the respective molar masses. These conversion factors ensured consistency between the chemical composition of the fertilizer solutions, which were then encoded in the nutrient composition matrix B, and the required elemental concentrations defined by the nutrient bounds in the model.

2.2.2. Optimal control problem

The control objective is to minimize the amount of fertilizer and water used during lettuce production while maintaining the nutrient concentrations within acceptable ranges, thereby avoiding both toxicity and deficiency of individual macronutrients in the solution. These acceptable ranges are defined in Table 2 and can be expressed as the following upper and lower bounds on the nutrient concentration:

$$C_m^{min} \le C_{m,t} \le C_m^{max}, \forall m \in \{1,2,\cdots,M\}, \forall t \in \{1,2,\cdots,T\} \quad (4)$$

in which $C_{m,t}$ denotes the concentration of the nutrient m at time t, C_m^{max} is the upper limit for nutrients m, and C_m^{min} is the lower limit for the nutrient m (see Table 2) for six macronutrients ($M = 6$). The nutrient concentration is defined as the ratio between the nutrient mass $x_{m,t}$ and the water volume $x_{7,t}$:

$$C_{m,t} = \frac{x_{m,t}}{x_{7,t}} \quad (5)$$

This definition of concentration is used to rearrange the constraints in Eq. (4) in terms of the states $x_{m,t}$ and $x_{7,t}$.

$$x_{7,t} {}^* C_m^{min} \le x_{m,t} \le x_{7,t} {}^* C_m^{max} \quad (6)$$

For compact representation, the inequality constraints in Eq. (6) for all species $m \in \{1,2,\cdots,M\}$, are represented in matrix form:

$$Ax_t \le 0 \quad (7)$$

in which matrix A contains the parameters C_m^{min} and C_m^{max}. To maintain feasibility in cases where strict adherence to these bounds may be unattainable, a vector of slack variables (s_t) was introduced into the optimization framework:

$$Ax_t \le s_t, s_t \ge 0 \quad (8)$$

- $s_t \in \mathbb{R}^{12}$, $t \in \{1,2,\cdots,T\}$: the slack variables to manage constraint softening.

The slack variable s_t can take nonnegative values, if required to ensure constraint satisfaction. However, a large penalty was applied to the non-zero values of s_t to ensure that this additional "slack" is avoided whenever possible. Eqs. (7) and (8) are expressed as linear inequality constraints.

We now formulate the optimal control problem using the dynamic model in Eq. (3), together with the slack variables introduced in Eq. (8). The objective includes a term penalizing the use of inputs u_t (the price of fertilizers and water) as well as a large penalty (quadratic) for non-zero slack variables s_t (indicating violation of the min/max concentrations of nutrients). All nutrient violations were penalized equally; that is, the cost of exceeding the upper bound (toxicity) is penalized the same way as falling below the lower bound (deficiency). The objective function is defined as the sum of these terms over the entire growing horizon ($t = 1, \cdots, T$). In the optimal control problem, the aim is to find the trajectory of inputs $u_1, u_2, \ldots, u_{T-1}$ and corresponding state trajectory $x_1, x_2, \ldots, x_T$, defined by the dynamical model, that minimized this objective function.

Table 2
Suitable lower and upper concentration bounds (in mg/L) for essential macronutrients in nutrient solution formulations and uptake rate in lettuce production (Albornoz and Lieth, 2016; Mattson and Peters, 2014).

Nutrient	Element	Lower bound (mg/L)	Upper bound (mg/L)	Range (mg/L)	Plant age and uptake rate (mg/g FW.day)			
					1–7 DAT	8–14 DAT	15–21 DAT	21–30 DAT
1	N	150	210	60	0.722 ± 0.032	0.603 ± 0.036	0.358 ± 0.033	0.209 ± 0.039
2	P	16	50	34	0.148 ± 0.002	0.214 ± 0.015	0.148 ± 0.004	0.324 ± 0.245
3	K	132	341	209	1.772 ± 0.101	1.794 ± 0.972	0.888 ± 0.202	0.303 ± 0.193
4	Ca	38	200	162	0.477 ± 0.090	0.376 ± 0.161	0.4 ± 0.179	0.471 ± 0.030
5	Mg	14	60	46	0.059 ± 0.008	0.092 ± 0.072	0.05 ± 0.016	0.133 ± 0.018
6	S	32	113	81	0.258 ± 0.098	0.323 ± 0.109	0.253 ± 0.196	0.297 ± 0.027

The optimization problem is expressed in the following standard formulation:

$$\min_{x,u,s} \sum_{t=1}^{T-1} c_u.u_t + \sum_{t=1}^{T} \|q_{s,t} \circ s_t\|_2^2 \tag{9}$$

$$s.t.$$

$$x_{t+1} = x_t + B.u_t + d_t \quad \forall t \in \{1, 2, \cdots, T-1\}$$

$$Ax_t \leq s_t \quad \forall t \in \{1, 2, \cdots, T\}$$

$$s_t \geq 0 \quad \forall t \in \{1, 2, \cdots, T\}$$

where c_u is the cost vector that includes the price of fertilizers and water (Table 1) and $q_{s,t}$ is the weight of the normalized allowable range of each nutrient (i.e., the difference between its upper and lower concentration limits, Table 2). Using this approach, nutrients with tight allowable ranges (stricter control requirements) received higher penalties for constraint violations, while nutrients with wider acceptable ranges were penalized less. This ensured the model treats all nutrients fairly and consistently without favoring those that naturally have higher concentration values. In the farm operation scenarios, Eq. (9) was subjected to further hard constraints (see Section 2.3). The optimization framework was implemented using CasADi (Andersson et al., 2019) and solved using the IPOPT solver in MATLAB, which is well-suited for large-scale problems involving convex quadratic programs.

2.2.3. Nutrient uptake uncertainty via Monte Carlo simulation

The plant nutrient–water uptake process is propagated through the optimal dosing policy using a Monte Carlo framework. For each simulation (a total of 20 simulations), a disturbance w_t was added to the nutrient uptake term on each day t from a bounded, element-wise uniform distribution, $w_t\ U[-a_{t,j}, a_{t,j}]$, with $a_{t,j}$ provided in Table 2. For every run, the decision trajectories and states were recorded. After all simulations, the mean and standard deviation across runs were computed and reported uncertainty using approximate two-sided 95% confidence intervals (CIs). Statistical comparisons among the baseline and optimized scenarios were conducted using two-sample t-tests. Effect sizes were quantified using Cohen's d, and significance was assigned at $p < 0.05$.

2.3. Scenario modeling

To evaluate the effect of nutrient dosing strategies, five distinct scenarios were developed and simulated to assess nutrient and water input strategies under varying operational constraints and grower behaviors.

2.3.1. Baseline scenario design and implementation

To evaluate system performance under minimal intervention, a baseline scenario was defined by imposing hard constraints on the dosing schedule. Specifically, all nutrient and water inputs were applied exclusively on the first day of the growing cycle, with no further applications permitted thereafter. Mathematically, the constraint added to Eq. (9), as follows:

$$u_t = 0, \forall t \in \{2, 3, \cdots, 30\} \tag{10}$$

These constraints simulated a single-shot fertigation strategy, whereby the entire required resources were delivered at the initiation of the growth period. The objective of this scenario is to assess the system's capacity to maintain optimal nutrient and nutrient solution levels throughout the 30-day cycle solely from an initial dose, without any subsequent control intervention. This approach serves as a reference point for evaluating the robustness of the system under extreme input limitations and highlights the temporal dynamics of nutrient availability and uptake under non-recurring fertigation regimes.

2.3.2. Scenario 1: Daily fertigation without constraints on water and fertilizer storage capacity

In this scenario, a dynamic fertigation strategy was implemented, wherein nutrient and water inputs were optimized and applied daily over a 30-day growing cycle. The aim was to evaluate the potential of dynamic, time-resolved dosing to maintain optimal system performance while minimizing resource input and constraint violations. Accordingly, no hard constraints were imposed on the capacities of the water and fertilizer tanks, allowing the optimization framework to explore the full range of feasible dosing strategies without being constrained by infrastructure limitations (Eq. (9)).

2.3.3. Scenario 2: Alternate-day fertigation without constraints on water and fertilizer storage capacity

A limited intervention fertigation strategy was explored, where nutrient and water dosing were only permitted on alternate days throughout the 30-day crop cycle. This constraint reflects practical limitations in some production systems, such as labor availability, automation cycles, or a desire to reduce fertigation frequency while still meeting crop needs. To implement the alternate-day dosing strategy, additional constraints were added to Eq. (9) to forbid any nutrient or water application on even-numbered days:

$$u_t = 0, \forall t \in \{2, 4, 6, \cdots, 30\} \tag{11}$$

This ensures that dosing was only allowed on odd-numbered days (i.e., 1, 3, 5, …, 29), effectively halving the number of intervention opportunities. This constraint was implemented directly within the optimization problem, ensuring that the solver accounted for non-dosing days when optimizing the dosing schedule. This alternate-day strategy evaluates the system's resilience to less frequent fertigation and explores whether adequate nutrient levels can still be maintained. It also supports evaluating trade-offs between dosing frequency, input use efficiency, and crop nutritional risk (deficiencies or toxicities) under limited intervention conditions.

2.3.4. Scenario 3: Daily fertigation under volume-constrained nutrient solution supply

Additional hard constraints were imposed to simulate practical limitations on the volume of nutrients in the solution in a closed-loop reservoir system. This approach reflected real-world CEA conditions, where fertigation systems have limited tank capacity and dosing equipment volume restrictions. This scenario introduced two critical physical constraints related to volume handling:

Reservoir volume constraint: The total solution volume in the reservoir (represented by the state variable x_7) was bound to remain within operational limits:

$$50 \leq x_{7,t} \leq 100, \ \forall t \in \{1, 2, \cdots, 30\} \tag{12}$$

These bounds reflect the minimum and maximum allowable volumes in the system's nutrient reservoir. Specifically, 50 L ensures a sufficient solution for the pump to operate, while 100 L represents the reservoir's upper limit to prevent overflow or system failure.

Fertilizer dosing volume constraint: The volume of fertilizer solution that can be injected into the reservoir per day was capped at 2 L across all nutrient components:

$$u_{i,t} \leq 2, \ \forall i \in \{1, 2, \cdots, 6\} \tag{13}$$

This constraint reflected the dosing pump's physical capacity or standard operational protocols, ensuring the system delivered precise, manageable amounts of concentrated nutrient solutions daily. Water dosing (represented by $u_{7,k}$) was not restricted by the 2-liter dosing cap, as it represents bulk volume that may be delivered through a different pumping system (Tank A to F).

2.3.5. Scenario 4: Alternate-day dosing under volume-constrained nutrient solution supply

The physical constraints from Scenario 3 were integrated with a reduced dosing frequency to simulate a volume-constrained alternate-day fertigation strategy. This scenario reflected a practical operational context where fertigation systems have limited reservoir capacity and dosing hardware. Dosing is scheduled every other day—e.g., due to automation schedules, resource conservation, or labor limitations. Thus, in addition to the constraints mentioned in scenario 3, dosing was only allowed on odd-numbered days. This was enforced by explicitly constraining the dosing vector to zero on all even-numbered days:

$$u_t = 0, \forall t \in \{2, 4, \cdots, 30\} \tag{14}$$

Thus, the constraints formulated in Eqs. (12), (13), and (14) were applied to Eq. (9) in Scenario 4. This scenario reduced the number of dosing opportunities by half (similar to Scenario 2), requiring the model to optimize nutrient delivery less frequently while still meeting plant demand and maintaining concentrations within target bounds. Table 3 provides a summary of the scenarios evaluated in this study.

2.4. Performance metrics

To assess the efficacy of each nutrient dosing strategy, a suite of quantitative performance metrics was employed encompassing agronomic, environmental, and economic dimensions.

Water use efficiency (WUE) was calculated as the ratio of total fresh biomass produced to the cumulative volume of water applied throughout the growing cycle (Eq. (15)). This metric reflects the ability of each dosing scheme to translate water input into harvestable yield, thereby serving as a proxy for irrigation efficiency.

$$\mathrm{WUE} = \frac{\textit{Fresh biomass}(g)}{\textit{Applied water}(L)} \tag{15}$$

Fertilizer use efficiency (FUE), defined as the total biomass produced per unit mass of fertilizer applied (Eq. (16)), was used to evaluate the effectiveness of nutrient delivery strategies. Higher FUE values indicate more efficient conversion of fertilizer input into crop output, reducing waste and environmental loading.

$$\mathrm{FUE} = \frac{\textit{Fresh biomass}(g)}{\textit{Applied fertilizer}(g)} \tag{16}$$

To quantify the adequacy of nutrient availability over time, two dimensionless composite indicators were introduced: the toxicity index (TI) and the deficiency index (DI). These indices reflected the cumulative deviation of nutrient concentrations from their agronomically acceptable bounds throughout the crop cycle, provided in Table 2. Together, these indices provide an integrated measure of nutrient imbalance, which can lead to growth inhibition, yield reduction, or physiological stress.

$$\mathrm{TI} = \frac{1}{MT}\sum_{m=1}^{M}\sum_{t=1}^{T}\max\left\{0, \frac{C_{m,t} - C_m^{max}}{C_m^{max}}\right\} \tag{17}$$

$$\mathrm{DI} = \frac{1}{MT}\sum_{m=1}^{M}\sum_{t=1}^{T}\max\left\{0, \frac{C_m^{min} - C_{m,t}}{C_m^{min}}\right\} \tag{18}$$

where $C_{m,t}$ is the actual concentration of the nutrient m at the time step t, C_m^{max} is the upper threshold (toxicity limit) of the nutrient n, C_m^{min} is the lower threshold (deficiency limit) of the nutrient m, T is the total number of time steps during the growing period ($T = 30$), and M is the number of nutrients considered ($M = 6$).

In addition to resource use efficiency and nutritional balance, the economic cost of nutrient solution management was estimated per kilogram of lettuce produced. This included both water and fertilizer inputs. Water cost was calculated assuming high-purity reverse osmosis water, priced at €3.10 per cubic meter (Gil et al., 2024) and converted to USD ($) using a fixed exchange rate of 1.10 (as listed on April 10, 2025). Fertilizer costs were based on a market price of $5.00 per pound for each of the six fertilizer types advertised by Green Leaf Aquarium (USA) and converted into cost per gram. These metrics enabled a comprehensive evaluation of trade-offs between input efficiency, crop performance, and operational cost under each scenario.

Table 3
Description of water and fertilizer dosing scenarios evaluated in *OptiDose* for optimization-based fertigation systems with individual macronutrient control.

Scenario	Description	Fertigation frequency	Operational constraints
Baseline	All fertilizers and water applied only on day 1; no subsequent intervention allowed throughout the 30-day cycle.	One-time (Day 1 only)	Hard constraint: no dosing after Day 1 ($u_t = 0, \forall t \in \{2,\ldots,30\}$)
Scenario 1	Fertilizers and water dosing with unrestricted tank capacity and dosing volumes.	Daily (Days 1–30)	No constraints on reservoir or pump capacity
Scenario 2	Fertilizers and water dosing allowed only on odd-numbered days to mimic limited intervention systems.	Alternate days (1, 3, 5, … 29)	Dosing forbidden on even days ($u_t = 0, \forall t \in \{2, 4,\ldots,30\}$)
Scenario 3	Fertilizers and water dosing under realistic physical constraints for reservoir and dosing volumes.	Daily (Days 1–30)	Reservoir volume bounds: $50 \le x_{7,t} \le 100$ L; Fertilizer dosing cap: $u_{i,t} \le 2$ L per fertilizer tank
Scenario 4	Fertilizers and water dosing every other day with volume-limited reservoir and pumps.	Alternate days (1, 3, 5, … 29)	Reservoir volume bounds; Fertilizer dosing cap; Dosing forbidden on even days ($u_t = 0, \forall t \in \{2,4,\ldots,30\}$)

3. Results and discussion

3.1. Temporal nutrient dynamics

Fig. 4 presents the resulting nutrient concentration profiles over a 30-day growing cycle, covering six essential macronutrients: N, P, K, Ca, Mg, and S. Each subplot includes dashed lines denoting optimal concentration ranges (Table 2), within which nutrient supply is presumed to meet plant requirements without inducing toxicity or deficiency.

The implemented optimal control strategy for the baseline scenario resulted in the complete depletion of all nutrients to their respective lower recommended thresholds on the harvesting day, except for Ca. Notably, the optimal initial nutrient concentrations were not aligned with the upper recommended thresholds, except for P, highlighting a more efficient starting formulation. Thus, in the absence of further dosing (baseline scenario), the optimal initial concentrations for the nutrient solution were determined to be 172 ± 3 mg/L for N, 50 ± 0 mg/L for P, 217 ± 14 mg/L for K, 160 ± 3 mg/L for Ca, 26 ± 2 mg/L for Mg, and 67 ± 5 mg/L for S, prepared in 14.3 ± 1.8 L of water per lettuce head. To achieve this composition, a total of 1,747 ± 182 g of fertilizers was dissolved in 960 ± 122 L of reverse osmosis water. The formulation consisted of 883 ± 117 g calcium nitrate, 260 ± 18 g magnesium sulfate, 218 ± 28 g monopotassium phosphate, 278 ± 19 g potassium nitrate, and 108 ± 13 g potassium sulfate, with no contribution from magnesium nitrate. The formulation and corresponding fertilizer tank configuration using six selected stock solutions are illustrated in Table 1 and Fig. 1.

Element-specific analysis revealed differential sensitivity of nutrients to the imposed fertigation strategies and constraints (Fig. 4). N, characterized by its high mobility and relatively wide sufficiency window,

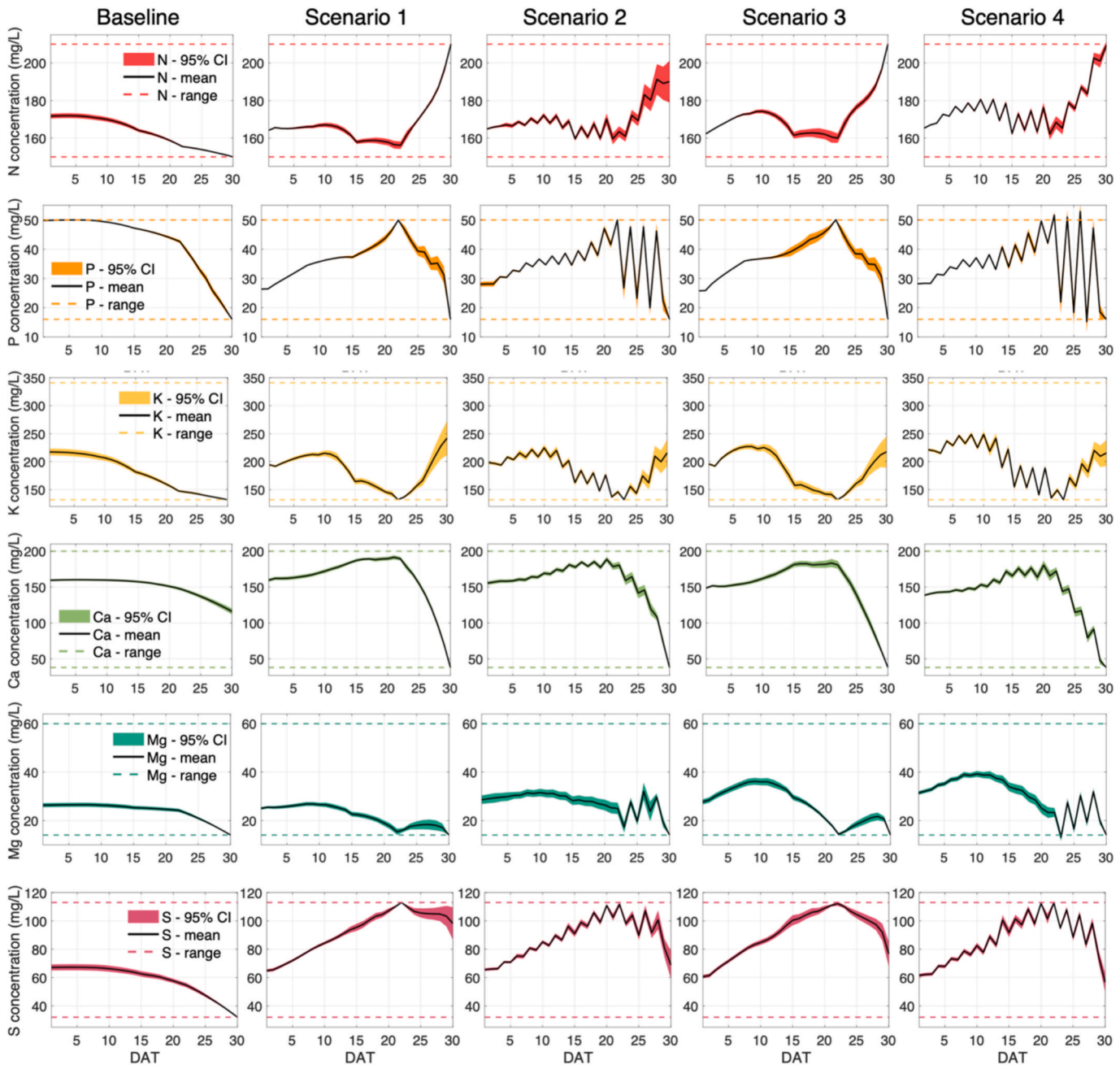

Fig. 4. Temporal dynamics of nutrient concentrations during a 30-day lettuce cultivation cycle under baseline and optimized dosing strategies with Monte Carlo uncertainty analysis (n = 20). Concentrations of nitrogen (N), phosphorus (P), potassium (K), calcium (Ca), magnesium (Mg), and sulfur (S) are shown for the baseline (static nutrient solution preparation) and Scenarios 1–4 (dynamic, element-based optimization strategies). Solid lines represent mean concentration, shaded areas indicate 95% confidence intervals, and dashed lines show the targeted sufficiency ranges for each nutrient.

was consistently maintained within optimal bounds across all dynamic scenarios. In contrast, P, Mg, and S, which exhibit narrower tolerance ranges and steeper uptake kinetics, were more prone to severe fluctuations, particularly in Scenario 4, yet resulted in low occurrence of violation (neither deficiency nor toxicity).

Notably, the implementation of Scenarios 1 to 4 substantially altered the initial P concentrations compared to the baseline, while concentrations of other nutrients remained largely unaffected at the outset. Alternate-day fertigation strategies (Scenarios 2 and 4) induced greater temporal variability, particularly for P, during the final week of the crop cycle. This was attributed to elevated late-stage P demand and the narrow range between P's upper and lower threshold values. Consequently, these scenarios appeared more susceptible to P imbalances, either deficiency or toxicity during the last growth stage.

Interestingly, all dynamic scenarios concluded with Ca concentrations approaching the lower sufficiency threshold, in contrast to the baseline scenario. Conversely, N concentrations at harvest consistently approached the upper threshold. K and Mg dynamics closely mirrored those observed under baseline conditions, indicating relative stability under varying dosing schedules.

Scenario 4, which combined alternate-day dosing with strict volumetric constraints, produced the largest oscillations in nutrient concentrations. Noticeable fluctuations, particularly for P, Mg, and S, arose because the system maintained the nutrient solution volume (Fig. 5) near the maximum allowable threshold (100 L), thereby increasing buffer capacity and acting as a low-pass filter that tried to attenuate

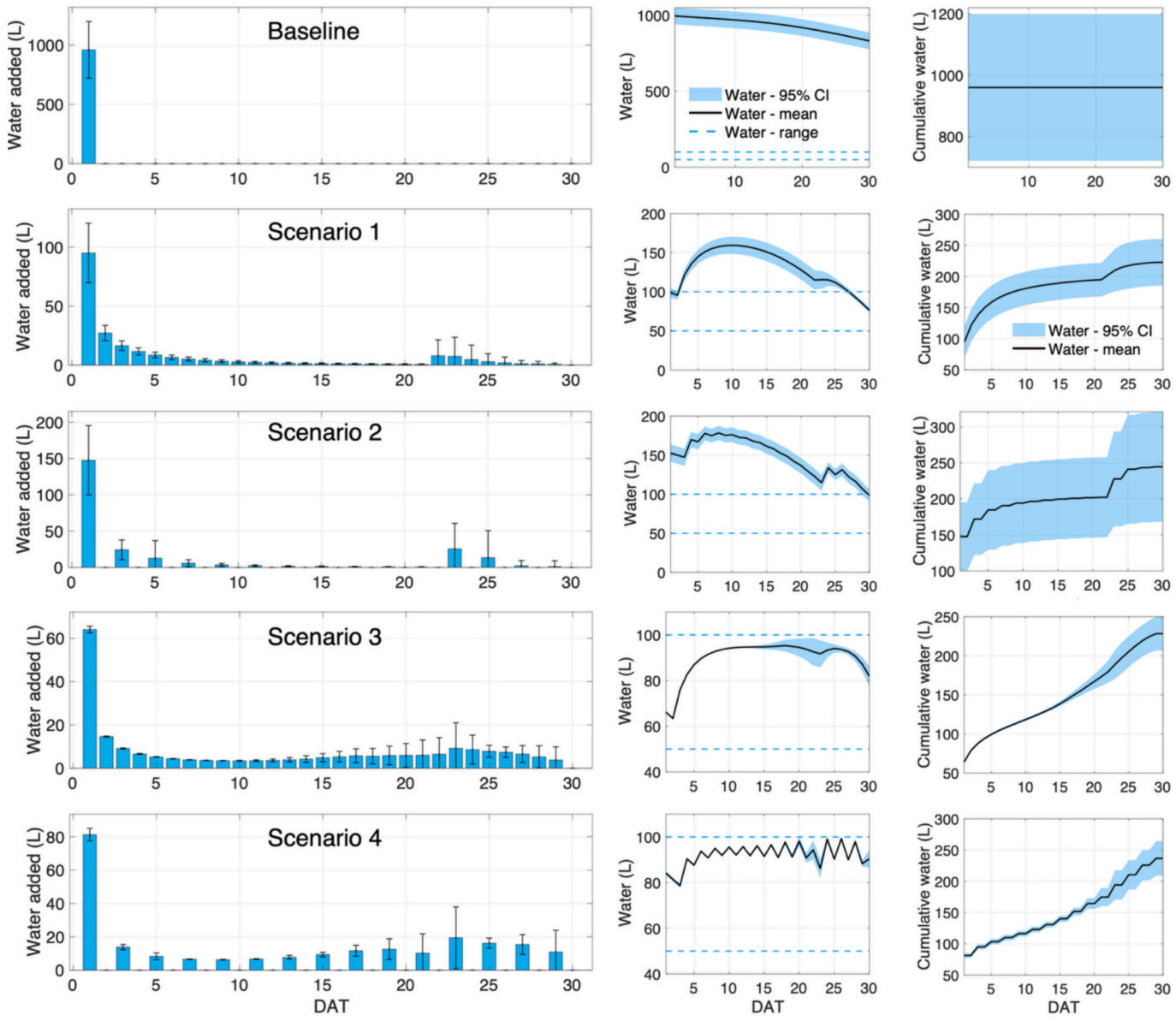

Fig. 5. Dynamic water management under various nutrient delivery scenarios. Water dynamics are illustrated across five strategies over a 30-day cultivation period. Left panels: Daily volume of water added to maintain nutrient solution levels, Middle panels: Temporal fluctuation of total water volume (nutrient solution) within the system. Right panels: Cumulative water consumption. Error bars represent the standard deviation.

sharp changes while ensuring sufficient nutrient mass to meet plant demand. Conversely, operating close to the minimum allowable volume (50 L) reduced this buffering effect and proved insufficient to simultaneously accommodate steep uptake rates of P, Mg, and S while keeping concentrations within the recommended bounds. In contrast, Scenario 3 permitted greater volumetric flexibility, and solution volumes tended to decline toward the minimum threshold.

Considering all scenarios, the *OptiDose*-derived formulation for initiating optimal lettuce growth converged on nutrient concentrations of 166 ± 4 mg/L N, 32 ± 10 mg/L P, 205 ± 13 mg/L K, 152 ± 9 mg/L Ca, 28 ± 2 mg/L Mg, and 64 ± 3 mg/L S. The comparatively high variability observed for P reflects the scenario-specific dynamics of nutrient uptake and water replacement. The *OptiDose* nutrient recipe values are consistently lower than those prescribed in the classical Hoagland solution (Hoagland and Arnon, 1938)—representing reductions of 27% in N, 14% in K, 5% in Ca, and 21% in Mg—yet remain broadly aligned with more recent recommendations (Resh, 2022; Soufi et al., 2023), exhibiting deviations of +16% for N, –5% for K, +45% for Ca, +14% for Mg, and +45% for S. In contrast, the OptiDose-derived optimal nutrient formulation required substantial deviations from the nutrient concentrations recently recommended for lettuce cultivation at an EC of 1.2 dS/m (Vought et al., 2024). Specifically, *OptiDose* identified markedly higher optimal concentrations of N and Ca, which increased by approximately 43% and 52%, respectively, relative to the concentrations prescribed in the EC 1.2 dS/m formulation. By comparison, the optimal Mg concentration was nearly reduced by half (28 ± 2 mg/L versus ~55 mg/L). In contrast, the *OptiDose* concentrations of K and P (~205 and ~32 mg/L) closely aligned with those specified in the EC 1.2 dS/m nutrient solution.

Beyond absolute nutrient concentrations, competitive interactions among Ca, K, and Mg warrant careful consideration. Excessive Ca accumulation can competitively inhibit the uptake of other cationic nutrients by reducing their access to shared transport and binding sites at the root interface (Vought et al., 2024). In particular, elevated Ca availability may suppress Mg uptake. Consequently, close monitoring and optimization of K:Ca:Mg ratios are essential to maintain balanced

nutrient acquisition and avoid cation antagonism (Meselmani, 2023).

It is also important to emphasize that preparing the *OptiDose* optimal formulation depends on the water volume allocated in each scenario. Because fertilizer application is ultimately governed by the total mass of nutrients delivered rather than their nominal solution concentrations, adherence to the scenario-specific water dosing schedule is essential to meeting the crop's actual nutrient demand throughout the growth cycle. For example, in deep-water culture (DWC) hydroponic systems—where plant roots are continuously submerged in a comparatively large, static volume of nutrient solution—Ca and K concentrations have been reported to remain relatively stable (Yang and Kim, 2019). This stability is primarily attributed to the greater buffering capacity of DWC systems, resulting from the larger absolute mass of dissolved nutrients, when compared with NFT systems.

3.2. Optimizing resource use under precision nutrient management scenarios

In the baseline scenario, *OptiDose* demonstrated that allocating ~14.3 ± 1.8 L of water per lettuce head (Fig. 5), combined with a nutrient formulation comprising 12.6 ± 1.7 g of calcium nitrate, 3.7 ± 0.3 g of magnesium sulfate, 3.1 ± 0.4 g of potassium phosphate, 4.0 ± 0.3 g of potassium nitrate, and 1.5 ± 0.2 g of potassium sulfate (totaling 25.0 ± 2.6 g of fertilizer; Fig. 6), was sufficient to complete the lettuce growth cycle without inducing either nutrient toxicity or deficiency. Notably, magnesium nitrate was identified as a redundant input (zero dosing) in this configuration, indicating that optimal crop performance can be achieved using a reduced set of five fertilizer types.

The baseline water allocation in our system was roughly five times higher than values reported for optimized DWC systems. In an optimized indoor, non-recirculating DWC setup for lettuce (*Lactuca sativa L. var. crispa*), a DLI of 12 mol/m^2/d and 3 L of nutrient solution per plant maximized biomass production and N and P removal (uptake) over a 35-day cycle (Aires et al., 2023). In our Scenario 4—the minimum-water strategy—the per-plant nutrient use (3.2 ± 0.1 L) closely matched this benchmark. However, fertilizer requirements differed markedly as the optimized DWC system used ~6.45 g per plant, whereas Scenario 4 required nearly 90% more.

3.2.1. Water dosing

The evapotranspiration rate of 2.5 L per lettuce head was observed. However, the baseline approach identified ~11.9 ± 2.6 L per head as the residual nutrient solution (wastewater) by the end of the growing cycle. While potentially reusable, this surplus introduces additional considerations related to wastewater treatment and associated costs, particularly in closed-loop hydroponic systems.

In contrast, Scenario 1 demonstrated the feasibility of producing lettuce with substantially improved water use efficiency. The peak solution volume achieved during the growth cycle (159 ± 25 L) delineates the minimum reservoir capacity required to ensure stable nutrient availability. In this case, the maximum water volume required during the cycle thus defines the optimal size of the nutrient reservoir. By starting the growing cycle with an initial reservoir of 1.4 ± 0.2 L per plant and replenishing the solution incrementally throughout the cultivation period (Fig. 5), total water use was reduced to 3.2 ± 0.1 L per plant—approximately 45% lower than the ion-ratio–based dosing strategy reported by Gang et al. (2025) for a 62-day greenhouse lettuce (Batavia and Romaine types) production in NFT. Their study maintained target macronutrient ratios using continuous ISE monitoring for N, K, and Ca, supplemented with weekly laboratory analyses for P, S, and Mg, with nutrient solution adjustments made twice weekly and a constant daily water addition. Also, water consumption in Scenario 1 was ~16% lower than the EC-based and plant-based nutrient management strategies evaluated by Soufi et al. (2023) during greenhouse cultivation of 42-day lettuce (*Lactuca sativa* var. *crispa*) in NFT.

Transitioning to an alternate-day dosing strategy with unrestricted access to water and nutrients (Scenario 2), however, resulted in a higher initial water requirement, which was ~56% greater than that observed in Scenario 1 (Fig. 5). A similar trend was observed in Scenarios 3 and 4 (Fig. 5), where more restrictive dosing frequencies and nutrient concentrations further shaped the dynamics of water and fertilizer utilization. In Scenarios 3 and 4, the water volume in the tank was permitted to fluctuate between 50 and 100 L. However, the actual operational ranges varied, spanning 64–100 L in Scenario 3 and 79–100 L in Scenario 4.

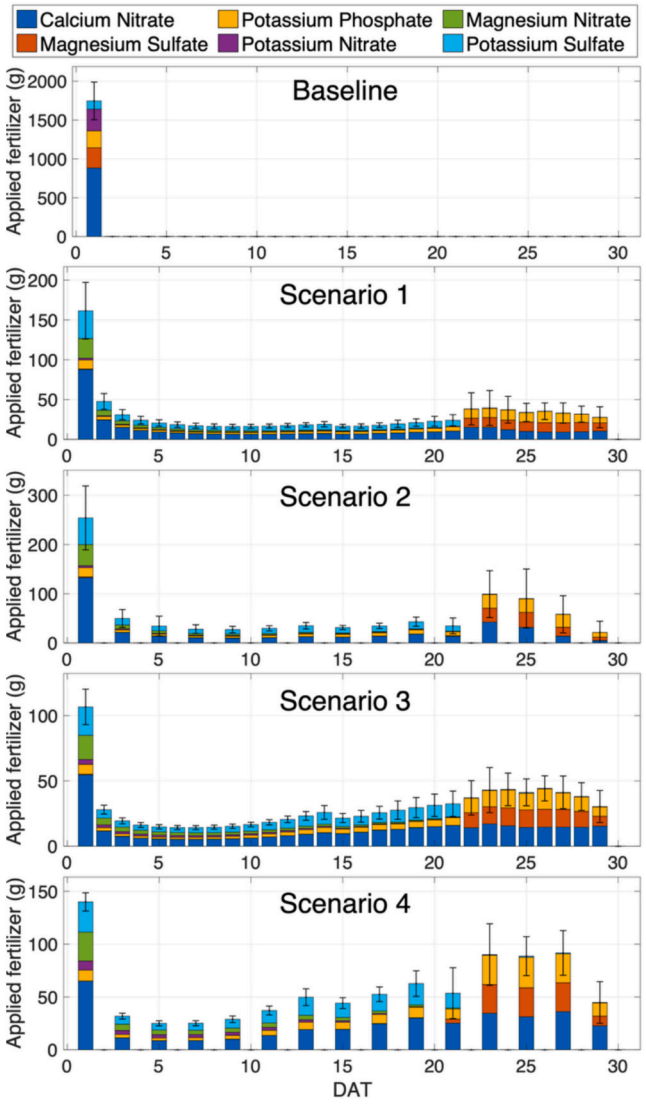

Fig. 6. Daily fertilizer application across the baseline and four optimized fertigation scenarios over a 30-day lettuce production cycle. Fertilizer dosing amounts (grams) are shown for six key macronutrient sources. Error bars indicate the standard deviation across all Monte-Carlo simulations (n = 20), reflecting uncertainty arising from variability in plant uptake demand.

Fig. 5 shows that the baseline scenario relies on a static single-shot input at day 1, with a slow decline in nutrient solution volume and no further water adjustments, indicating inefficiencies in both control and response. In contrast, Scenarios 1–4 demonstrate active and responsive water management, characterized by frequent small-volume additions. These findings highlight the substantial impact of farmer-selected nutrient management strategies on optimizing resource use efficiency.

3.2.2. Fertilizer dosing

The cumulative fertilizer application across Scenarios 1–4 was ~50% lower than the baseline, demonstrating that informed on-farm

management strategies in hydroponic production can markedly reduce nutrient inputs. Such improvements in fertilizer-use efficiency have broader implications, as they highlight the potential for advanced hydroponic management to mitigate a portion of the current ~398 million tons of CO_2-equivalent emissions annually from global fertilizer manufacturing (Ren and Rosa, 2025).

Baseline management followed a static, one-time application strategy with extremely high initial input, particularly calcium nitrate (~883 ± 117 g), and no further additions. In contrast, Scenarios 1–4 adopt dynamically adjusted dosing strategies, distributing fertilizer applications in smaller quantities throughout the crop cycle. Scenario 1 applied frequently, low-dose inputs across all nutrients, whereas Scenario 2 combined early-stage pulses with mid-to-late cycle boosts, suggesting stage-specific nutrient demand targeting. Scenario 3 exhibited a gradual ramp-up of consistent, low-level inputs, whereas Scenario 4 displayed a more adaptive pattern with variable fertilizer sources, particularly after day 20.

Fertilizer redundancy patterns varied across the scenarios. While magnesium nitrate was dispensable in the baseline configuration, potassium nitrate emerged as redundant in Scenarios 1 and 2 (Fig. 6). In contrast, under stricter nutrient input constraints in Scenarios 4 and 5, all fertilizers were utilized, suggesting a tighter margin for optimization. Across all cases, calcium nitrate consistently represented the highest share of applied nutrients, underscoring its pivotal role in lettuce cultivation (Fig. 6). It is important to note that the fertilizer dosing prescriptions in this study differ from those reported by Gang et al. (2025), primarily due to differences in problem definition and study objectives, with the latter focusing on the maintenance of ionic balance. A similar difference in dosing was observed in Jung et al. (2019), attributable to their use of fixed set-point concentrations for specific ions, in contrast to the range of allowable concentrations considered in the present study.

3.3. Water and fertilizer consumption and efficiency

The baseline scenario, representative of conventional static fertigation practices, resulted in the highest total water and fertilizer input across the 30-day cultivation period. Notably, this input strategy yielded the lowest WUE at 5.8 ± 0.9 g/L and FUE at 6.1 ± 0.7 g/g, indicating inefficient resource utilization and potential over-application losses (Table 4) in comparison to literature (Barbosa et al., 2015). The baseline system also generated 831 ± 126 L of wastewater, more than eight times that of the following highest scenario.

In contrast, Scenarios 1–4, each utilizing dynamic, optimized fertigation algorithms, achieved an average WUE of 28.6–32.3 g/L, a significant ($p < 0.05$) and nearly 6-fold increase compared to the baseline (Table 4). Similarly, FUE values stabilized ~12 g/g, effectively doubling the efficiency of fertilizer conversion into biomass (Table 4). This performance is comparable to that of a highly advanced, leaf-turgor-pressure-based closed-loop aeroponic system tested on romaine lettuce (*Lactuca sativa L. var. longifolia*) over a 37-day cycle, which reported a WUE of ~28 g/L (Karnoutsos et al., 2025). In contrast, optimized lettuce production under ebb-and-flow conditions—using a Hoagland nutrient solution, an 85% lower field-capacity irrigation threshold, and supplemental ozone at 1 mg/L—reported markedly higher resource-use efficiencies, with WUE and FUE reaching 40.1 g/L and 58.9 g/g, respectively, for a 37-day lettuce grown (*Lactuca sativa L.*) at a DLI of ~8.7 mol/m^2/d and an EC of 2.2 dS/m (Zhao et al., 2024). These elevated efficiencies may be partly explained by differences in environmental drivers. Specifically, the substantially lower DLI in their system (~8.7 mol/m^2/d) relative to NFT conditions in this research (14.4 mol/m^2/d), together with higher vapor-pressure deficit, which lead to elevated crop evapotranspiration, thereby increasing water and nutrient uptake dynamics. Additionally, WUE values of 28.1 g/L for ebb-and-flow systems and 52.9 g/L for aeroponics were reported (Carotti et al., 2023). However, these estimates account for total water use, including both irrigation inputs and water captured through climate-control processes, particularly the recovery of indoor moisture via heating, ventilation, and air-conditioning systems. Consequently, cross-study comparisons of WUE and FUE must be interpreted with caution, as methodological differences, system-level feedback, and varying definitions of "total resource use" can substantially influence the reported efficiencies.

Remarkably, all scenarios, including the baseline, achieved near-zero average nutrient deficiency (DI) and toxicity (TI), confirming that optimal control dosing strategies did not compromise crop nutrient status despite reduced input levels (Table 4). This behavior raised from the quadratic penalty functions applied to deviations beyond the upper and lower concentration bounds for each nutrient in the cost function (Eq. (9)). In practice, *OptiDose* mitigated the likelihood of deficiency or toxicity by strategically adjusting fertilizer dosing—and, more prominently, water additions—to minimize these boundary violations. Meanwhile, as the operating constraints become more stringent—particularly in Scenarios 3 and 4—nutrient imbalances increasingly manifest as deficiencies rather than toxicities. This shift likely reflects the cost structure embedded in the optimization framework, whereby the penalty associated with additional fertilizer inputs biases the algorithm toward solutions that tolerate mild deficiencies rather than risk excessive nutrient application. Baseline strategy applied inputs far in excess of actual crop needs, and that dynamic, model-based management can maintain optimal crop performance yet at substantially lower environmental and economic costs.

3.4. Economic implications

Economic analysis further supported the advantages of the optimized approaches. The total cost of nutrient solution (combined water and fertilizer) in the baseline was 2.2 ± 0.1 USD/kg, compared to 0.98–1.00

Table 4
Performance of different nutrient and water optimization strategies compared to a baseline scenario. Metrics include total water and fertilizer consumption, wastewater generation, average nutrient deficiency and toxicity index, resource use efficiency (water and fertilizer), and associated costs.

Optimization strategy	Total water used (L)	Total wastewater (L)	Total fertilizer used (g)	DI (−)	TI (−)	WUE (g/L)	FUE (g/g)	Water cost (USD/kg)	Fertilizer cost (USD/kg)
Baseline	960 ± 126a	831 ± 126a	1747 ± 182a	0	0	5.8 ± 0.9a	6.1 ± 0.7a	0.33 ± 0.04a	1.83 ± 0.19a
Scenario 1	223 ± 7b (*, d = −8.5)	76 ± 7b (*, d = −8.5)	857 ± 24b (*, d = −6.0)	0	0	32.3 ± 1.4b (*, d = +3.4)	12.3 ± 0.3b (*, d = +10.1)	0.08 ± 0.00b (*, d = −9.0)	0.90 ± 0.03b (*, d = −7.0)
Scenario 2	245 ± 18b (*, d = −6.1)	99 ± 18b (*, d = −6.1)	871 ± 27b (*, d = −5.5)	0	0	28.6 ± 2.6c (*, d = +2.9)	12.1 ± 0.4b (*, d = +9.0)	0.09 ± 0.01b (*, d = −6.5)	0.91 ± 0.03b (*, d = −6.8)
Scenario 3	228 ± 10b (*, d = −7.9)	82 ± 10b (*, d = −7.9)	858 ± 24b (*, d = −6.0)	0.01 ± 0.03	0.00 ± 0.01	31.3 ± 1.8b (*, d = +3.3)	12.2 ± 0.4b (*, d = +9.3)	0.08 ± 0.00b (*, d = −9.0)	0.90 ± 0.02b (*, d = −7.2)
Scenario 4	237 ± 9b (*, d = −8.1)	90 ± 9b (*, d = −8.1)	866 ± 24b (*, d = −5.9)	0.70 ± 0.49	0.23 ± 0.14	29.7 ± 1.5c (*, d = +3.1)	12.1 ± 0.3b (*, d = +10.4)	0.09 ± 0.00b (*, d = −9.1)	0.91 ± 0.03b (*, d = −7.0)

Mean ± standard deviation (n = 20). Superscripts (a–c) indicate grouping from post-hoc Tukey tests ($p < 0.05$). Asterisk (*) indicates significance level relative to the baseline strategy ($p < 0.05$). Cohen's d values describe standardized effect sizes.

USD/kg in optimized Scenarios 1–4, a 55% reduction in total input cost. This significant ($p < 0.05$) reduction is largely driven by the reduced fertilizer usage, with fertilizer costs halving from 1.83 ± 0.19 USD/kg in the baseline to approximately 0.90–0.91 USD/kg in the other optimized treatments. Additionally, due to decreased total irrigation volumes, water costs dropped from 0.33 ± 0.04 USD/kg in the baseline to 0.08–0.09 USD/kg in all other optimized scenarios. Accordingly, the transition from the baseline to Scenario 1 resulted in significant ($p < 0.05$) reductions in water and fertilizer costs, by ~76% and ~51%, respectively. Such reductions in operational input could substantially improve farmers' profit margins, thereby enhancing the economic viability of CEA. However, the labor costs and/or expenses associated with autonomous hardware required to implement strategies 1–4 were not included in this analysis.

3.5. Uncertainty analysis

The Monte Carlo simulations highlighted the critical role of feedback control in maintaining nutrient sufficiency under uncertain plant uptake. During early growth (DAT 0–10), all strategies showed stable nutrient profiles with narrow confidence intervals, reflecting low uptake variability and reduced nutrient demand. However, as lettuce entered rapid growth (DAT 15–30), uncertainty in nutrient uptake widened the 95% confidence intervals (Fig. 4). The baseline strategy exhibited the highest variability in both nutrient and water dynamics, with a total fertilizer SD of 182 g and water SD of 126 L, driven primarily by sharp fluctuations in calcium nitrate demand (SD = 117 g). In contrast, Scenarios 1–4 achieved lowest overall variability (total SD = 24 g), reflecting greater dosing stability under constrained operational limits. This stability likely arises from the reduced solution volume, which necessitated smaller total fertilizer inputs and restricted the flexibility of dosing adjustments, thereby narrowing the operational space and enforcing a more rigid—yet stable—control pathway.

Water use showed higher relative uncertainty (defined as $SD/mean \times 100$) compared to nutrient concentrations in the baseline (13%), Scenario 1 (19%), and Scenario 2 (15%), despite ignoring evapotranspiration uncertainties. *OptiDose* appeared to dynamically propagate uncertainties in macronutrient uptake into the water dosing strategy, as the penalization of the slack variable effectively constrains both overshooting and undershooting of individual nutrient targets. In practice, the capacity to modulate solution volume functions as a low-pass filter, attenuating fluctuations in nutrient mass uptake while maintaining concentrations within agronomically suitable ranges. Furthermore, the substantially lower cost of water could be an additional reason. This variability was markedly reduced in Scenarios 3 and 4 due to hard volume constraints (50–100 L), although these restrictions led to occasional nutrient imbalances during high-demand phases (DAT 15–30).

Nutrient-level uncertainty patterns were varied by nutrient and growth stage. N exhibited the lowest relative uncertainty (1% in baseline), while Mg showed the highest (15% in Scenario 2), reflecting its sensitivity to uptake fluctuations. Temporal uncertainty peaked near the end of the growth cycle (DAT 27), with P variability reaching 52%, coinciding with rapid nutrient uptake during late vegetative growth. These findings underscore the need to incorporate feedback-enabled control strategies or more advanced optimal control frameworks—such as model predictive control (MPC)—capable of dynamically compensating for disturbances and model–system mismatches. Evidence from aquaponic systems demonstrates the efficacy of such approaches (Debroy et al., 2025). This enhances system stability, reliability, and overall operational resilience under a wide range of conditions. Alternatively, increasing the temporal resolution of nutrient monitoring during periods of rapid plant demand may provide a pragmatic pathway to maintain solution stability and ensure accurate nutrient delivery.

3.6. Study limitations and future direction

The application of optimal control in this study demonstrated the ability to dynamically and precisely manage water and six selected fertilizer inputs, thereby maintaining target concentrations of macronutrients (N, P, K, Ca, Mg, and S) across all five scenarios, even under strict operational constraints. Despite this promising performance, several limitations warrant careful consideration to guide future implementations.

First, the *OptiDose* results can be sensitive to the accuracy of evapotranspiration and nutrient uptake models, which are strongly influenced by plant biomass and environmental conditions. In this study, evapotranspiration was assumed to follow a fixed relationship with biomass; however, in real-world applications, evapotranspiration is driven by complex interactions among temperature, vapor pressure deficit, wind speed, CO_2 concentration, and light intensity—whether from solar radiation, artificial lighting, or a combination thereof—in controlled environments. These interactions not only influence water demand but also modulate daily biomass accumulation. Integrating machine learning models to predict evapotranspiration and biomass accumulation using environmental data and computer vision tools may improve model fidelity and reduce uncertainty.

Moreover, the uptake rates used in this study were based on literature values that may not fully capture the inherent variability introduced by nutrient synergies and antagonisms in the root zone (Niu et al., 2015; Vought et al., 2024; Zhang et al., 2010). The dynamic interplay of ions in solution was not considered particularly under fluctuating environmental conditions. Nutrient absorption rates can vary substantially due to physiological stages, environmental stressors, and interactions within the root-zone solution. For example, uptake values reported by Albornoz and Lieth (2016) suggested that ammonium (NH_4) and nitrate (NO_3) exhibit the highest uncertainties in uptake, particularly in later growth stages. These nitrogen species are also more sensitive to environmental and physiological changes than other macronutrients, such as K and Mg, which displayed more consistent uptake patterns. This work aggregated N into a single form, potentially oversimplifying its behavior. Future optimization frameworks should consider the individual dynamics of NO_3-N and NH_4-N to enhance dosing precision and reduce the risk of toxicity or deficiency, given the recommended NH_4 to NO_3 ratio of 20:80 (corresponding to a total nitrogen concentration of 100 mg/L; Xu et al., 2025). During plant growth, roots not only absorb water and nutrients but also release protons, inorganic ions, and low-molecular-weight organic compounds that alter rhizosphere pH and nutrient availability, thereby influencing nutrient uptake dynamics (Dakora and Phillips, 2002). This rhizosphere-driven feedback was not accounted for in this study. Incorporating real-time pH monitoring would enable correction of nutrient-uptake values. Our model assumes spatially uniform nutrient concentration along each channel and therefore does not capture micro-scale heterogeneity. Additionally, salt precipitation in irrigation pipelines and potential emitter clogging were not considered in this analysis.

While *OptiDose* scheduled dosing based on predicted uptake, it did not incorporate feedback from real-time analysis of the nutrient solution. Regular sampling and chemical analysis of nutrients in the hydroponic solution could enable feedback control, reduce drift and correcting for modeling errors, thereby improving robustness. Validation of the proposed simulations under real-world conditions is crucial for evaluating the effectiveness of the recommended control ranges and optimization strategies.

The current cost function in the formulation accounted for fertilizer costs and penalties for exceeding toxicity or deficiency thresholds (Eq. (9)). However, other relevant cost drivers, such as labor for dosing events or the final-day volume of unused nutrient solution, were not considered. Expanding the objective function to include these parameters may allow tailoring of the optimization for economic or environmental performance, depending on farmer priorities. Moreover, the

slack variables in Eq. (9) assigned equal weights to nutrient toxicity and deficiency. Future research could refine this framework by introducing differentiated penalty weights according to the relative importance of specific nutrients and experimental objectives. For instance, Eq. (9) could be reformulated to impose a higher penalty on N toxicity relative to S deficiency, or assign a greater weighting to Ca deficiency to prioritize quality traits (e.g., reducing the risk of tip-burn; Li et al., 2025), thereby aligning the optimization with crop-specific sensitivities or management priorities. Under such a formulation, the optimal control problem would yield tailored fertigation schedules that maintain consistency with the intended experimental design throughout the growing cycle.

The modular nature of *OptiDose* enables the extension to micronutrients and the incorporation of redundancy in fertilizer selection. Future studies are encouraged to explore whether increased redundancy, achieved through multiple sources of the same nutrient and various nutrient combinations, either improves or compromises system efficiency, cost-effectiveness, and environmental sustainability. Furthermore, while this study focused on lettuce in a hydroponic system, the approach is extensible to other crops in CEA, and it may be applicable to open-field systems with some adaptation. Successful implementation in diverse contexts will require robust modeling of evapotranspiration, crop-specific nutrient uptake, water-nutrient dynamics in the growing medium, and, most importantly, effective feedback mechanisms.

The present study utilized a single water source (reverse osmosis) to simulate the optimization of nutrients and irrigation. However, the proposed *OptiDose* framework is inherently adaptable and can be extended to accommodate multiple water sources with varying physicochemical properties. This feature allows for the development of more comprehensive and context-specific fertigation strategies. Future research should investigate the integration of water sources with diverse quality profiles, along with their associated costs per cubic meter, to further refine the optimization model and enhance its applicability under real-world constraints.

Lastly, a key contribution of this study is the advancement of element-based nutrient management through the *OptiDose* framework, which enables precise control of fertilizer application and water use in hydroponic systems. By optimizing dosing strategies at the elemental macronutrient level, *OptiDose* strengthens the principles of precision agriculture, improving nutrient-use efficiency while minimizing waste and potential environmental impacts. Despite the limitations discussed, the framework establishes a solid foundation for next-generation automated fertigation, with clear potential for integration into hardware platforms for real-time solution management. Furthermore, by systematically evaluating hydroponic recipes within defined concentration thresholds, *OptiDose* provides a robust decision-support tool for maintaining consistent nutrient supply. Collectively, these innovations underscore the novelty of the approach and highlight its relevance for developing more resilient and resource-efficient CEA systems.

4. Conclusion

Transitioning from conventional EC-based control to individual nutrient management is pivotal in achieving closed-loop, zero-waste hydroponic systems. This study presented an optimal control framework named *OptiDose*, developed to optimize water and macronutrient (N, P, K, Ca, Mg, and S) dosing in hydroponic lettuce production. By simulating five distinct farm management scenarios, *OptiDose* demonstrated its ability to dynamically regulate nutrient concentrations within recommended nutrient range while enhancing resource use efficiency. The implementation of individualized daily fine-tuning of water and fertilizer inputs significantly ($p < 0.05$) increased water use efficiency from 5.8 ± 0.9 to 32.3 ± 1.4 g/L and fertilizer use efficiency from 6.1 ± 0.7 to 12.3 ± 0.3 g/g compared with single-shot nutrient-solution preparation. Additionally, the associated costs of water and fertilizer inputs were significantly ($p < 0.05$) reduced from 0.33 ± 0.04 to 0.08 ± 0.00 USD/kg and from 1.83 ± 0.19 to 0.90 ± 0.03 USD/kg, respectively. Across all scenarios, *OptiDose* successfully reduced overall fertigation costs while ensuring that macronutrient concentrations remained within agronomically suitable thresholds, thereby avoiding both deficiencies and toxicities for plants. These findings confirm that an optimal control framework enables precise nutrient-based fertigation control (overcoming the limitations of EC-based approaches), which can be flexibly applied to diverse hydroponic production systems.

CRediT authorship contribution statement

Saeed Karimzadeh: Writing – review & editing, Writing – original draft, Visualization, Validation, Software, Project administration, Methodology, Investigation, Funding acquisition, Formal analysis, Data curation, Conceptualization. **Robert D. McAllister:** Writing – review & editing, Validation, Supervision, Methodology, Conceptualization. **Md Shamim Ahamed:** Writing – review & editing, Supervision, Resources.

Declaration of competing interest

The authors declare the following financial interests/personal relationships which may be considered as potential competing interests: Saeed Karimzadeh reports financial support was provided by Drainage Foundation sr. If there are other authors, they declare that they have no known competing financial interests or personal relationships that could have appeared to influence the work reported in this paper.

Acknowledgements

S.K. acknowledges the partial support provided by the Drainage Foundation sr through the AdaptCrop project.

Appendix A. Supplementary data

Supplementary data to this article can be found online at https://doi.org/10.1016/j.compag.2026.111428.

Data availability

The dataset used to model lettuce growth dynamics in this study is publicly available at https://doi.org/10.5281/zenodo.17041810. All computational codes for data processing, modeling, and analysis were developed in MATLAB (R2024b Update 3, version 24.2.0.2806996, 64-bit, macOS) and are available from Saeed Karimzadeh upon reasonable request.

References

Afram, A., Janabi-Sharifi, F., 2014. Theory and applications of HVAC control systems – a review of model predictive control (MPC). Build. Environ. 72, 343–355. https://doi.org/10.1016/j.buildenv.2013.11.016.

Ahamed, M.S., Chowdhury, M., Sarwar Inam, A.K.M., Kar, K.A., Islam, M.N., Karimzadeh, S., Tabassum, S., Kabir, M.S., Akter, N., Momin, A., 2025. A comprehensive review of advances in sensing and monitoring technologies for precision hydroponic cultivation. Comput. Electron. Agric. 237, 110601. https://doi.org/10.1016/j.compag.2025.110601.

Aires, L.M.I., Ispolnov, K., Luz, T.R., Pala, H., Vieira, J.S., 2023. Optimization of an indoor DWC hydroponic lettuce production system to generate a low N and P content wastewater. Processes 11 (2), 365. https://doi.org/10.3390/pr11020365.

Albornoz, F., Lieth, J.H., 2016. Daily macronutrient uptake patterns in relation to plant age in hydroponic lettuce. J. Plant Nutr. 39 (10), 1357–1364. https://doi.org/10.1080/01904167.2015.1109110.

Ali Al Meselmani, M. (2023). Nutrient Solution for Hydroponics. In M. Turan, S. Argin, E. Yildirim, & A. Güneş (Eds), *Recent Research and Advances in Soilless Culture*. IntechOpen. https://doi.org/10.5772/intechopen.101604.

Andersson, J.A.E., Gillis, J., Horn, G., Rawlings, J.B., Diehl, M., 2019. CasADi: a software framework for nonlinear optimization and optimal control. Math. Program. Comput. 11 (1), 1–36. https://doi.org/10.1007/s12532-018-0139-4.

Bailey, B.J., Haggett, B.G.D., Hunter, A., Albery, W.J., Svanberg, L.R., 1988. Monitoring nutrient film solutions using ion-selective electrodes. J. Agric. Eng. Res. 40 (2), 129–142. https://doi.org/10.1016/0021-8634(88)90110-2.

Barbosa, G., Gadelha, F., Kublik, N., Proctor, A., Reichelm, L., Weissinger, E., Wohlleb, G., Halden, R., 2015. Comparison of land, water, and energy requirements of lettuce grown using hydroponic vs. conventional agricultural methods. Int. J. Environ. Res. Public Health 12 (6), 6879–6891. https://doi.org/10.3390/ijerph120606879.

Carotti, L., Pistillo, A., Zauli, I., Meneghello, D., Martin, M., Pennisi, G., Gianquinto, G., Orsini, F., 2023. Improving water use efficiency in vertical farming: Effects of growing systems, far-red radiation and planting density on lettuce cultivation. Agric Water Manag 285, 108365. https://doi.org/10.1016/j.agwat.2023.108365.

Catota-Ocapana, P., Minaya-Andino, C., Astudillo, P., Pichoasamin, D., 2025. Smart control models used for nutrient management in hydroponic crops: a systematic review. IEEE Access 13, 13070–13087. https://doi.org/10.1109/ACCESS.2025.3526171.

Cho, W.J., Kim, H.-J., Jung, D.H., Kang, C.I., Choi, G.-L., Son, J.-E., 2017. An embedded system for automated hydroponic nutrient solution management. Trans. ASABE 60 (4), 1083–1096. https://doi.org/10.13031/trans.12163.

Christofides, P.D., Scattolini, R., Muñoz De La Peña, D., Liu, J., 2013. Distributed model predictive control: a tutorial review and future research directions. Comput. Chem. Eng. 51, 21–41. https://doi.org/10.1016/j.compchemeng.2012.05.011.

Dakora, F.D., Phillips, D.A., 2002. Root exudates as mediators of mineral acquisition in low-nutrient environments. In: Adu-Gyamfi, J.J. (Ed.), Food Security in Nutrient-Stressed Environments: Exploiting Plants' Genetic Capabilities. Springer, Netherlands, pp. 201–213. https://doi.org/10.1007/978-94-017-1570-6_23.

Debroy, P., Majumder, P., Seban, L., 2025. A simulation based water quality parameter control of aquaponic system employing model predictive control strategy incorporation with optimization technique. Environ. Prog. Sustain. Energy 44 (1), e14530. https://doi.org/10.1002/ep.14530.

Dela Vega, J.A., Gonzaga, J.A., Gan Lim, L.A., 2021. Fuzzy-based automated nutrient solution control for a hydroponic tower system. IOP Conf. Ser.: Mater. Sci. Eng. 1109 (1), 012064. https://doi.org/10.1088/1757-899X/1109/1/012064.

Ding, Y., Wang, L., Li, Y., Li, D., 2018. Model predictive control and its application in agriculture: a review. Comput. Electron. Agric. 151, 104–117. https://doi.org/10.1016/j.compag.2018.06.004.

Domingues, D.S., Takahashi, H.W., Camara, C.A.P., Nixdorf, S.L., 2012. Automated system developed to control pH and concentration of nutrient solution evaluated in hydroponic lettuce production. Comput. Electron. Agric. 84, 53–61. https://doi.org/10.1016/j.compag.2012.02.006.

Gang, M.-S., Kim, H.-J., Ahn, T.I., Cho, W.-J., Lee, S.-H., Lee, J.Y., Hwang, J.-E., 2025. Development of nutrient management system based on ion-equivalent concentration ratio and ion monitoring to maintain ionic balance in closed hydroponic solution. Comput. Electron. Agric. 237, 110588. https://doi.org/10.1016/j.compag.2025.110588.

Giannothanasis, E., Karavidas, I., Ntanasi, T., Ntatsi, G., Thompson, R.B., Savvas, D., 2025. Sodium accumulation management in a closed-loop soilless cropping system using ion selective electrodes and a novel decision support System. Smart Agric. Technol. 12, 101366. https://doi.org/10.1016/j.atech.2025.101366.

Giannothanasis, E., Spanoudaki, E., Kinnas, S., Ntatsi, G., Voogt;, W., Savvas, D., 2024. Development and validation of an innovative algorithm for sodium accumulation management in closed-loop soilless culture systems. Agric Water Manag 301, 108968. https://doi.org/10.1016/j.agwat.2024.108968.

Gil, J.D., González, R.A., Sánchez-Molina, J.A., Berenguel, M., Rodríguez, F., 2024. Reverse osmosis desalination for greenhouse irrigation: experimental characterization and economic evaluation based on energy hubs. Desalination 574, 117281. https://doi.org/10.1016/j.desal.2023.117281.

Grewal, H.S., Maheshwari, B., Parks, S.E., 2011. Water and nutrient use efficiency of a low-cost hydroponic greenhouse for a cucumber crop: an Australian case study. Agric Water Manag 98 (5), 841–846. https://doi.org/10.1016/j.agwat.2010.12.010.

Hoagland, D., Arnon, D. (1938). The water-culture method for growing plants without soil. Circular. California Agricultural Experiment Station, *347*, 39 pp. CABI Databases.

Jung, D.H., Kim, H.J., Choi, G.L., Ahn, T.I., Son, J.E., Sudduth, K.A., 2015. Automated lettuce nutrient solution management using an array of ion-selective electrodes. Trans. ASABE 1309–1319. https://doi.org/10.13031/trans.58.11228.

Jung, D.-H., Kim, H.-J., Cho, W.-J., Park, S.H., Yang, S.-H., 2019. Validation testing of an ion-specific sensing and control system for precision hydroponic macronutrient management. Comput. Electron. Agric. 156, 660–668. https://doi.org/10.1016/j.compag.2018.12.025.

Kamilaris, A., Prenafeta-Boldú, F.X., 2018. Deep learning in agriculture: a survey. Comput. Electron. Agric. 147, 70–90. https://doi.org/10.1016/j.compag.2018.02.016.

Karimzadeh, S., Ahamed, M.S., 2025. Lettuce dataset with RGB canopy images, biomass, nutrient solution, and environmental variables for machine learning model development. Zenodo. https://doi.org/10.5281/ZENODO.17041810.

Karimzadeh, S., Ahmadi, A., Baldocchi, D., Fisher, J.B., 2025a. Climate change has increased global evaporative demand except in South Asia. Commun. Earth Environ. 6 (1), 1009. https://doi.org/10.1038/s43247-025-02959-x.

Karimzadeh, S., Daccache, A., Rulli, M.C., Ahamed, M.S., 2025b. Global water-nutrient-salinity-energy nexus in lettuce production: from open-field irrigation to closed-loop hydroponics in greenhouses. J. Agric. Food Res. 21, 101935. https://doi.org/10.1016/j.jafr.2025.101935.

Karimzadeh, S., Li, Z., Ahamed, M.S., 2025c. Machine learning-based fault detection and diagnosis of electrical conductivity and pH sensors in hydroponic systems. Comput. Electron. Agric. 237, 110544. https://doi.org/10.1016/j.compag.2025.110544.

Karnoutsos, P., Katsantonis, D., Gkotzamani, A., Koukounaras, A., Kotsopoulos, T., Pantazi, X.E., Fragos, V.P., 2025. Plant-driven precision irrigation in aeroponics: real-time turgor sensing for sustainable lettuce cultivation. Agriculture 15 (18), 1948. https://doi.org/10.3390/agriculture15181948.

Kim, J., Kim, H.-J., Gang, M.-S., Kim, D.-W., Cho, W.-J., Jang, J.K., 2023. Closed hydroponic nutrient solution management using multiple water sources. J. Biosyst. Eng. 48 (2), 215–224. https://doi.org/10.1007/s42853-023-00182-0.

Langenfeld, N.J., Pinto, D.F., Faust, J.E., Heins, R., Bugbee, B., 2022. Principles of nutrient and water management for indoor agriculture. Sustainability 14 (16), 10204. https://doi.org/10.3390/su141610204.

Li, Z., Karimzadeh, S., Chavanapanit, A., Moghimi, A., Ahamed, M.S., 2025. Detection of calcium deficiency in indoor-grown lettuce under LED lighting using computer vision. Smart Agric. Technol. 12, 101144. https://doi.org/10.1016/j.atech.2025.101144.

Mashumah, S., Rivai, M., Irfansyah, A.N., 2018. Nutrient film technique based hydroponic system using fuzzy logic control. Int. Seminar Intelli. Technol. Appl. (ISITIA) 2018, 387–390. https://doi.org/10.1109/ISITIA.2018.8711201.

Massa, D., Incrocci, L., Maggini, R., Bibbiani, C., Carmassi, G., Malorgio, F., Pardossi, A., 2011. Simulation of crop water and mineral relations in greenhouse soilless culture. Environ. Model. Software 26 (6), 711–722. https://doi.org/10.1016/j.envsoft.2011.01.004.

Mattson, N. S., & Peters, C. A. R. I. (2014). A recipe for hydroponic success. *Inside Grower*, *2014* (Jan), 16-19.

Mohamed, B.T., Ahmed, A.M., Ahmed, A.A., Omar, Y.K., Makram, A.M., Fouad, K.K., Soliman, A.A., Abo-Elmagd, A.M., 2022. Smart hydroponic system using fuzzy logic control. In: 2022 2nd International Mobile, Intelligent, and Ubiquitous Computing Conference (MIUCC), pp. 189–194. https://doi.org/10.1109/MIUCC55081.2022.9781654.

Niu, Y., Jin, G., Li, X., Tang, C., Zhang, Y., Liang, Y., Yu, J., 2015. Phosphorus and magnesium interactively modulate the elongation and directional growth of primary roots in *Arabidopsis thaliana* (L.) Heynh. J. Exp. Bot. 66 (13), 3841–3854. https://doi.org/10.1093/jxb/erv181.

Nizam, N.A.I.M., Chung, S.K., Yew, H.T., Kiring, A.M.J., 2024. Hydroponic IoT-based control using adaptive fuzzy, PID, and consensus control methods for nutrient concentration dosing. J. Phys. Conf. Ser. 2928 (1), 012001. https://doi.org/10.1088/1742-6596/2928/1/012001.

C. Nurmahaludin J. Riadi Nutrient concentration control system in hydroponic plants based on fuzzy logic Int. Conf. Appl. Sci. Technol. (iCAST) 2020 2020 141 146 10.1109/iCAST51016.2020.9557617.

Pandey, K., Singh, K.G., Singh, A., 2023. Multi-Sensors based smart nutrient reuse management system for closed soilless culture under protected cultivation. Comput. Electron. Agric. 204, 107495. https://doi.org/10.1016/j.compag.2022.107495.

Puno, J.C.V., Haban, J.J.I., Alejandrino, J.D., Bandala, A.A., Dadios, E.P., 2020. Design of a Nutrient Film Technique Hydroponics System with Fuzzy Logic Control. In: 2020 IEEE REGION 10 CONFERENCE (TENCON), pp. 403–408. https://doi.org/10.1109/TENCON50793.2020.9293749.

Rahman, M.K.I.A., Buyamin, S., Abidin, M.S.Z., Mokji, M.M., 2018. Development of automatic mixing process for fertigation system in rock melon cultivation. Int. J. Electr. Comput. Eng. (IJECE) 8 (3), 1913. https://doi.org/10.11591/ijece.v8i3.pp1913-1919.

Raviv, M., Lieth, J.H., Bar-Tal, A., 2019. Significance of Soilless Culture in Agriculture. In: Soilless Culture. Elsevier, pp. 3–14. https://doi.org/10.1016/B978-0-444-63696-6.00001-3.

Ren, C., Rosa, L., 2025. Global energy and carbon emissions of irrigation and fertilizers management for closing crop yield gaps. Environ. Res. Lett. 20 (10), 104026. https://doi.org/10.1088/1748-9326/adfbfd.

Resh, H.M. (2022). Hydroponic food production: a definitive guidebook for the advanced home gardener and the commercial hydroponic grower (8th edn). CRC Press. https://doi.org/10.1201/9781003133254.

Savvas, D., Giannothanasis, E., Ntanasi, T., Karavidas, I., Drakatos, S., Panagiotakis, I., Neocleous, D., Ntatsi, G., 2023. Improvement and validation of a decision support system to maintain optimal nutrient levels in crops grown in closed-loop soilless systems. Agric Water Manag 285, 108373. https://doi.org/10.1016/j.agwat.2023.108373.

Soufi, H.R., Roosta, H.R., Hamidpour, M., 2023. The plant growth, water and electricity consumption, and nutrients uptake are influenced by different light spectra and nutrition of lettuce. Sci. Rep. 13 (1), 20766. https://doi.org/10.1038/s41598-023-48284-1.

Steidle Neto, A.J., Zolnier, S., De Carvalho Lopes, D., 2014. Development and evaluation of an automated system for fertigation control in soilless tomato production. Comput. Electron. Agric. 103, 17–25. https://doi.org/10.1016/j.compag.2014.02.001.

Trejo-Téllez, I., Gómez-Merino, F.C. (2012). Nutrient Solutions for Hydroponic Systems. In T. Asao (Ed.), Hydroponics—A Standard Methodology for Plant Biological Researches. InTech. https://doi.org/10.5772/37578.

Vought, K., Bayabil, H.K., Pompeo, J., Crawford, D., Zhang, Y., Correll, M., Martin-Ryals, A., 2024. Dynamics of micro and macronutrients in a hydroponic nutrient film technique system under lettuce cultivation. Heliyon 10 (11), e32316. https://doi.org/10.1016/j.heliyon.2024.e32316.

Xu, J., Che, G., Yan, J., Luo, Y., Good, A., Yuan, T., Lei, Z., Zhang, Z., Shizumi, K., 2025. Optimizing nitrogen form ratio for enhanced nutrient uptake and lettuce performance in hydroponic systems. Bioresour. Technol. Rep. 32, 102384. https://doi.org/10.1016/j.biteb.2025.102384.

Ya-Gang Wang, Zhi-Gang Shi, Wen-Jian Cai. (2001). PID autotuner and its application in HVAC systems. Proceedings of the 2001 American Control Conference. (Cat. No.01CH37148), 2192–2196 vol.3. https://doi.org/10.1109/ACC.2001.946075.

Yang, T., Kim, H.-J., 2019. Nutrient management regime affects water quality, crop growth, and nitrogen use efficiency of aquaponic systems. Sci. Hortic. 256, 108619. https://doi.org/10.1016/j.scienta.2019.108619.

Zhang, F., Niu, J., Zhang, W., Chen, X., Li, C., Yuan, L., Xie, J., 2010. Potassium nutrition of crops under varied regimes of nitrogen supply. Plant Soil 335 (1–2), 21–34. https://doi.org/10.1007/s11104-010-0323-4.

Zhang, R., Zhou, J., Feng, L., Ma, W., 2019. Study of variable liquid fertilization control system based on fuzzy PID control. In: Proceedings of the Conference on Research in Adaptive and Convergent Systems, pp. 67–70. https://doi.org/10.1145/3338840.3355642.

Zhao, Q., Guo, S., Feng, J., Li, D., Yang, S., Zhou, X., 2024. Suitable water–fertilizer management and ozone synergy can enhance substrate-based lettuce yield and water–fertilizer use efficiency. Agronomy 14 (8), 1619. https://doi.org/10.3390/agronomy14081619.